

Amperometric Assay of Sodium Dodecyl Sulfate Based on Anion Exchange Using PDDA as Active Acceptor

Zhong-Xia Wang, Yuan-Fei Gao, Xian-He Yu, Fen-Ying Kong, Wen-Juan Wang,
Wei-Xin Lv and Wei Wang*

School of Chemistry and Chemical Engineering, Yancheng Institute of Technology, Yancheng
224051, China.

*E-mail: wangw@ycit.edu.cn

Received: 12 May 2018 / Accepted: 13 June 2018 / Published: 5 August 2018

This study demonstrates a facile and effective strategy for amperometric assay of electrochemically inactive sodium dodecyl sulfate (SDS) based on different binding affinity of poly(diallyldimethylammonium chloride) (PDDA) toward electrochemically inactive SDS and active $[\text{Fe}(\text{CN})_6]^{3-/4-}$ anions. To improve conductivity of the modified electrode nanomaterial, PDDA/GO/SWCNTs hybrid nanomaterial is first prepared and used as the artificial receptor to recognize the anions (i.e., $[\text{Fe}(\text{CN})_6]^{3-/4-}$ and SDS). The stronger binding affinity of the PDDA toward SDS than $[\text{Fe}(\text{CN})_6]^{3-/4-}$ anions results in the decrease of the redox peaks current of surface modified PDDA and provides a quantitative signal readout for the SDS assay. Thereafter, an amperometric assay for SDS based on anion-exchange at $[\text{Fe}(\text{CN})_6]^{3-/4-}$ /PDDA/GO/SWCNTs modified glassy carbon electrode was developed. The ratio of the current decrease shows a linear relationship with SDS concentration range from 1.0 to 200 μM , and the limit of detection of SDS is 36.51 nM. And the results indicate that the study not only provides a simple and effective way to a polyanion of SDS assay, but also opens a new route to developing electrochemical methods for electrochemically inert contaminants by fully utilizing the anion-exchange principles.

Keywords: Poly(diallyldimethylammonium chloride); Differential pulse voltammograms; Electrochemically inactive; Anion-exchange; Sodium dodecyl sulfate;

1. INTRODUCTION

Sodium dodecyl sulfate (SDS), as a commonly used surfactant, has expanded from the chemical industry to all areas of our daily life in the past decades, and it is usually called the “industrial monosodium glutamate”. Although many methods provided degradation of technology for SDS, the considerable portion of residual surfactant still damage the aquatic ecosystems, drinking

water quality and even evoke intensive pollution of water reservoirs [1, 2]. So it is of crucial importance to monitor closely SDS levels in the aqueous solution for the sake of health. Recently, various traditional techniques and methods, including colorimetric, chromatographic, fluorescence, and biosensor analysis methods, have been developed to detect the SDS [3-7]. However, most of these techniques show some disadvantages which include expensive reagents, time-consuming analysis, complicated procedures, need sophisticated instrumentation, and the lack of specificity or potential interference from other factors. Therefore, it still remains a great challenge to establish a reliable, simple, sensitive, and selective analytical technique to detect SDS in the environment.

Electropolymerization of organic monomers provides a reproducible and controllable route to improve conductive surfaces at the nanometer level [8]. Poly(diallyldimethylammonium) chloride (PDDA), a cationic water-soluble polymer containing a large number of nitrogen-containing groups and as a commonly used electropolymerization of organic monomers, exhibits unique adsorption ability for different substances via electrostatic adsorption, such as carbon nanotubes [8, 9], and metal nanoparticles [10] to synthesize hybrid nanocomposite with unexpected features. Furthermore, PDDA, as a cationic polymer, is widely used to fabricate ultra-thin modified nanofilms through the method of layer-by-layer assembly using electrostatic attraction with anionic polymer. Accordingly, PDDA might be used as the medium for synthesis of high-performance electrochemical nanomaterials.

Herein, we proposed a facile yet effective amperometric method for the SDS assay with PDDA as the synthetic receptor, as shown in Scheme 1. The electropolymeric nanofilms of PDDA cationic surfactant and GO/SWCNTs hybrid nanocomposites was firstly used to electrostatically absorb $[\text{Fe}(\text{CN})_6]^{3-/4-}$ anions as electrochemical probe to prepare $[\text{Fe}(\text{CN})_6]^{3-/4-}/\text{PDDA}/\text{GO}/\text{SWCNTs}$ (FePGSs) modified glassy carbon electrode (GCE). Quite stable and well-defined redox peaks belonging to the confined $[\text{Fe}(\text{CN})_6]^{3-/4-}$ with negative shift potentials compared with the pure $[\text{Fe}(\text{CN})_6]^{3-/4-}$ in aqueous solution were observed at FePGSs/GCE. Furthermore, the anion-exchange of the small anions, $[\text{Fe}(\text{CN})_6]^{3-/4-}$ replace by polyanions, SDS at PDDA/GO/SWCNTs nanofilms was observed. By taking advantages of the large surface area and high electronic conductivity of GO/SWCNTs and reducing the overpotential effect of PDDA, an amperometric assay for SDS based on anion-exchange at FePGSs modified GCE was developed. To the best of our knowledge, the research undertaken here has not been reported so far and could offer a new path to fabrication of stable FePGSs nanofilm electrodes with excellent electrochemical properties of wide response range and low detection limit that are envisaged to be particularly useful for electrochemically inactive molecules studies and electroanalytical applications.

2. EXPERIMENTAL

2.1 Reagents and chemicals

Single-walled carbon nanotubes (SWCNTs, with surface area $40\text{-}300\text{ m}^2\text{ g}^{-1}$, average diameter of $\sim 1\text{-}5\text{ nm}$, and length of $10\text{-}20\text{ }\mu\text{m}$), graphite powder (GP, $<45\text{ }\mu\text{m}$, $\geq 99.99\%$) and poly(diallyldimethylammonium chloride) (PDDA) were obtained from Sigma-Aldrich. Sodium dodecyl sulfate (SDS), potassium ferricyanide and potassium ferrocyanide were obtained from

Shanghai Sinopharm Chemical Reagent Co. Ltd. (Shanghai, China). Phosphate buffered solution (PBS, pH 6.0-8.0, 50 mM) were prepared with Na_2HPO_4 and NaH_2PO_4 . Other chemicals were of at least analytical grade reagents and were used as received. Double distilled water was used throughout.

2.2 Apparatus

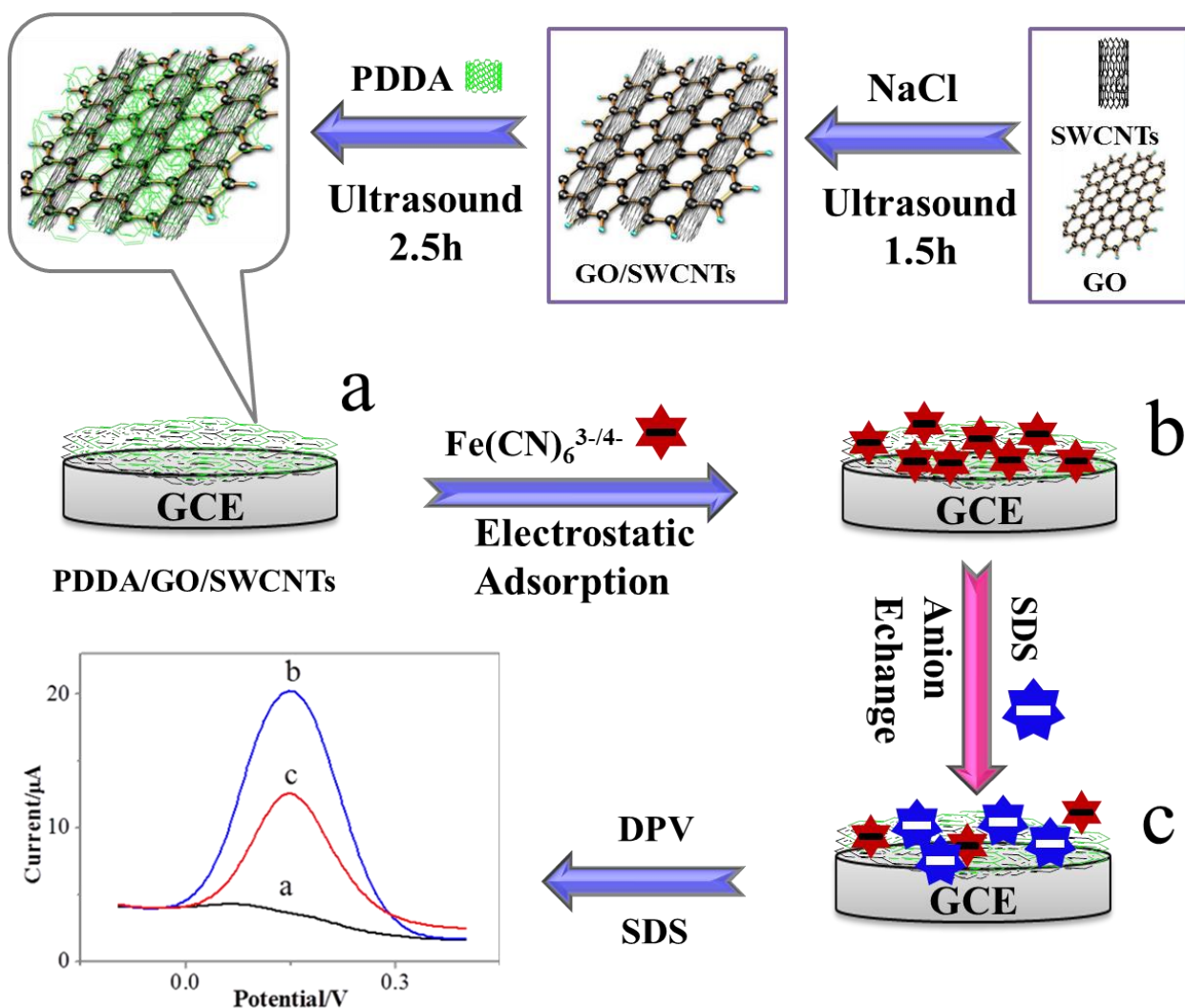
Electrochemical measurements experiments were carried out on a CHI 660E electrochemical workstation (Shanghai CH Instruments Co.) with a three-electrode configuration. A saturated calomel electrode (SCE) as reference electrode, a platinum wire (Pt) as counter electrode, and the nanomaterials modified glassy carbon electrode (GCE, diameter 3 mm) were used as working electrode. All potentials herein are referenced to the SCE. The morphology of the prepared GO, SWCNTs and PDDA/GO/SWCNTs nanocomposite, and the energy-dispersive X-ray spectroscopy (EDS) of the obtained nanocomposite were carried out using a FEI Sirion 200 scanning electron microscope (FEI).

2.3 Noncovalent functionalization of GO/SWCNTs by PDDA

GO were synthesized from graphite powder by a modified Hummer's method [11, 12]. And the procedure for synthesizing SWCNTs with more negatively charged was adapted from the method described by previous literature reported [13]. The step for the noncovalent functionalization of GO and SWCNTs using PDDA is as follows: briefly, 10.5 mg of SWCNTs and 10.5 mg of GO were mixed in 50 mL of 1.0 M NaCl solution to form a homogeneous solution. After the 50 mL as-prepared solution was sonicated for 1.5 h, and the 80 mg of PDDA was added. Then, the mixed solution was continuously sonicated for 2.5 h. Next, the resulting solution was centrifuged at 7000 rpm for 30 min to remove excess PDDA and NaCl. Finally, the product was resuspended in 5 mL distilled water. And the PDDA/GO/SWCNTs nanocomposites homogeneous suspension solution was obtained.

2.4 Fabrication of SDS sensor

Prior to the fabrication of the electrochemical sensor, GCE (3.0 mm in diameter) was first polished on emery paper, then with aqueous slurries of alumina powder (1.0, 0.3, and 0.05 μm) on a polishing cloth, cleaned ultrasonically with ethanol and water for 2 min, respectively, rinsed thoroughly with water and allowed to dry at room temperature. Then, 6.0 μL of PDDA/GO/SWCNTs nanocomposites was successively coated onto the working electrode and dried in the air. Hereafter, the PDDA/GO/SWCNTs-modified GCE were subjected to consecutive incubation in the 5 mM $[\text{Fe}(\text{CN})_6]^{3-/4-}$ solution for 15 min. The resulting electrodes (i.e., FePGSS/GCE) were rinsed three times with the double distilled water and finally dried at room temperature before carrying out the electrochemical measurements. For comparison, modified GCE electrode with GO/SWCNTs or PDDA was also prepared using the same procedure. All electrochemical measurements experiments were performed at 25 °C. And the fabrication of the FePGSSs modified electrode is shown in Scheme 1.



Scheme 1. The stepwise fabrication process of the SDS sensor.

2.5 Electrochemical measurements

The cyclic voltammetric (CV) and amperometric measurements were carried out on a CHI 660E potentiostat (Shanghai CH Instruments Co.). A conventional three-electrode configuration setup in 10 mL of 50 mM PBS solution, pH 7.0 at 25 °C was used, the PDDA/GO/SWCNTs nanocomposites, GO/SWCNTs and PDDA modified electrode as the working electrode, a platinum wire as the counter electrode, and SCE as the reference electrode.

For amperometric sensing of SDS, the FePGSs/GCE were first immersed in 50 mM PBS (pH 7.0) containing different concentrations of SDS for 15 min and then taken out of the solution and rinsed with ultrawater to remove the physically adsorbed SDS. The resulting electrode was subsequently immersed into the pure PBS solution (50 mM, pH 7.0) for the electrochemical determination.

3. RESULTS AND DISCUSSION

3.1 Characterization of PDDA/GO/SWCNTs nanocomposites

PDDA/GO/SWCNTs hybrid nanocomposite was directly synthesized by the one-step simple electrostatic adsorption between PDDA and GO/SWCNTs mixed solution. And the surface morphologies of SWCNTs, GO and GO coated SWCNTs by the intermediate medium of PDDA were observed by SEM, as shown the Figure 1. As can be seen from the Figure 1A, the SEM image of the pure SWCNTs shows that the SWCNTs are highly tangled with each other and have a smooth surface. And the Figure 1B shows the SEM image of pure GO, which has a nano-flower clusters shape, not a single layer structure. The reason may be attributed to the insufficient acidification. After incorporating PDDA into the GO and SWCNTs matrix (Figure 1C), the hybrid composite displays a 3D rough structure as unexpected, and the dense dispersion of SWCNTs on the surface of GO through the intermediate medium of PDDA was clearly observed, which endows lots of positively charged active sites and good conductivity of the PDDA/GO/SWCNTs nanocomposite, and indicates the successful formation of PDDA/GO/SWCNTs hybrid nanofilm by simple electrostatic adsorption process. In addition, the formation of PDDA/GO/SWCNTs hybrid nanofilm was further proven by the EDS spectrum, as shown in Figure 1D. From the Figure 1D, it is clear that three typical peaks are related to C, N and O elements, respectively, and containing N (9.15 wt%) element mainly from the PDDA polymer (Figure 1D).

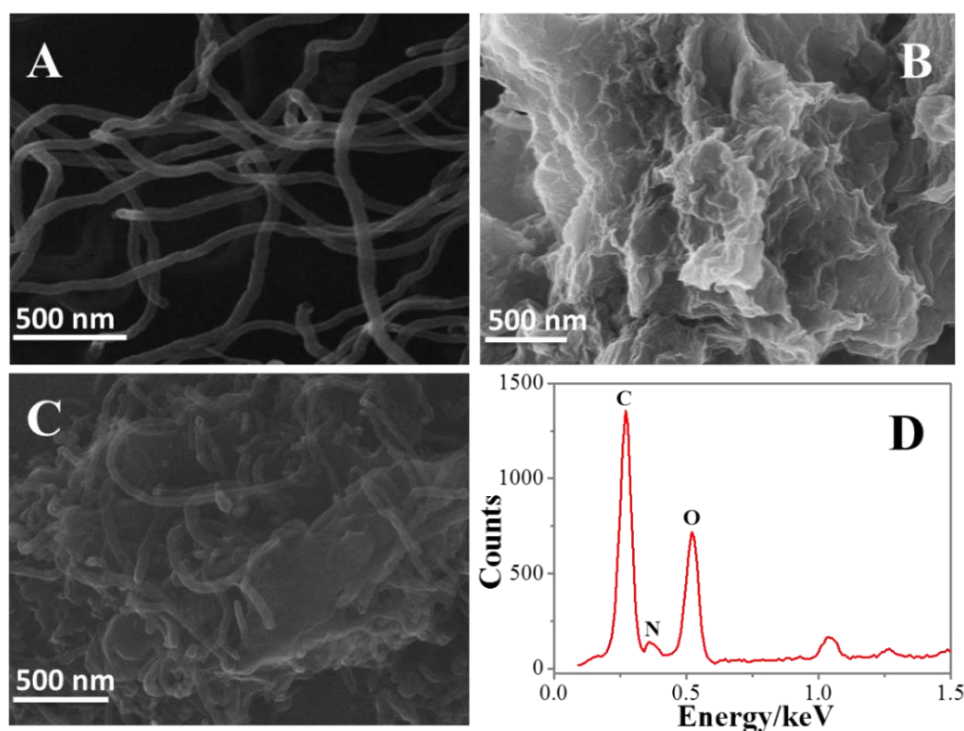


Figure 1. The SEM images of (A) SWCNTs, (B) GO, (C) PDDA/GO/SWCNTs, and EDS (D) of PDDA/GO/SWCNTs nanocomposite.

3.2 Electrochemical behaviors of confined FePGSs/GCE

CVs was used to demonstrate the electrode behaviors of the $[\text{Fe}(\text{CN})_6]^{3-/4-}$ markers in the confined state in the hybrid nano-films and its other state in aqueous solution at GO/SWCNTs, PDDA modified and bare GCE, since the electron transfer between the modified electrode and the solution species usually produce by tunneling either through the barrier or through the defects of electrode modified hybrid nano-films in the barrier [14]. Figure 2 shows the CVs of differently modified electrodes in 1.0 mM $[\text{Fe}(\text{CN})_6]^{3-/4-}$ containing 0.1 M KCl solution with a scan rate of 100 mV s^{-1} . As shown in Figure 2, compared with the bare GCE (Figure 2, curve a), the peak currents of GO/SWCNTs modified electrode increases lightly, indicating that the GO/SWCNTs markedly improve the electron transfer rate due to their unique properties of excellent conductivity (Figure 2, curve b) [15, 16]. For the PDDA/GCE (Figure 2, curve c), the cathodic and anodic peak currents increase slightly, which maybe attribute to the electrostatic attraction between the positive charge of PDDA and the negative probes. Meanwhile, it is important to note that the position of peak currents of the PDDA/GCE produces greatly negative shift, and the apparent peak potential ($E_p = (E_{pa} + E_{pc})/2$) negatively shifts $\sim 90 \text{ mV}$ compared with the bare GCE (Figure 2, curve a), indicating that for the PDDA-modified electrode, the PDDA can greatly reduce the overpotential in the catalytic ferricyanide-redox reaction.

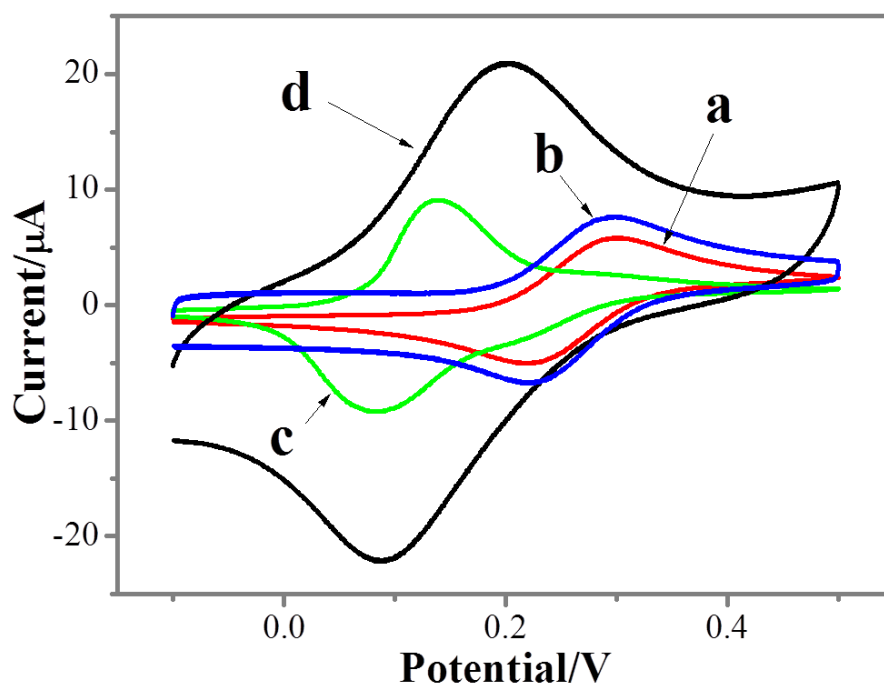


Figure 2. CVs obtained at bare GCE (a), GO/SWCNTs/GCE (b), PDDA/GCE (c) and PDDA/GO/SWCNTs/GCE (d) in 0.1 M KCl containing 1 mM $\text{K}_3\text{Fe}(\text{CN})_6/\text{K}_4\text{Fe}(\text{CN})_6$ (1:1) respectively.

What's more, the background and peak currents of the PDDA/GO/SWCNTs hybrid nano-films modified electrode increase greatly, and the apparent peak potential ($E_p = (E_{pa} + E_{pc})/2$) negatively shifts $\sim 75 \text{ mV}$ compared with bare GCE (Figure 2, curve a), indicating that the synergetic effect

between PDDA and GO/SWCNTs improves the capability of the electrocatalytic performance, resulting greatly reduced the overpotential and increased peak currents. Namely, the reason for the negative shift of PDDA/GO/SWCNTs hybrid nano-films modified electrode might contribute to the electrostatic attraction of the positive PDDA polymer and the negative probes. And the larger peak current at PDDA/GO/SWCNTs/GCE demonstrate the better electronic conductivity of PDDA/GO/SWCNTs nanofilm due to the introduction of GO/SWCNTs. Therefore, the electrocatalytic activity of the FePGSSs nanocomposite could be markedly improved because of the electron withdrawing ability of the N active site from the PDDA can create net positive charge on the adjacent carbon atoms in the PDDA/GO/SWCNTs nanocomposite plane [17, 18].

The synthesis procedure is illustrated in the Experimental Section. And the PDDA/GO/SWCNTs-modified electrode was prepared by primer method. The confined $[\text{Fe}(\text{CN})_6]^{3-/4-}$ was obtained by dipping the PDDA/GO/SWCNTs-modified electrode into 5 mM $[\text{Fe}(\text{CN})_6]^{3-}$ and $[\text{Fe}(\text{CN})_6]^{4-}$ mixture (1:1) for 15 min, respectively, washed thoroughly with double-distilled water and kept in a dry state for later use. To explore the electron transfer process, the influence of potential scan rate on the electrochemical behavior of FePGSSs modified GCE in the 50 mM PBS solution (pH 7.0) was investigated by CVs (Figure 3). It is seen that a pair of stable and well-defined quasi-reversible anodic and cathodic peaks are presented, which could be attributed to the surface adsorption of $[\text{Fe}(\text{CN})_6]^{3-/4-}$ anion [19], and with the increasing of scan rate from 5 to 200 mV s^{-1} , both the reduction and oxidation peaks currents were increased linearly (Figure 3B) and the peak to peak separation was 78 mV and nearly independent of the scan rate (Figure 3A), which revealed that the electrochemical reaction ability and electron transfer between FePGSSs and GCE could be easily performed at the FePGSSs nanofilm and it was a surface-controlled electrochemical process, not a diffusion-controlled electrochemical process [20]. These results indicate that the electro-conductibility of the containing N active site of FePGSSs nanocomposite would become dominant, and thus plays an important role in decreasing overpotential and facilitating the electron transfer.

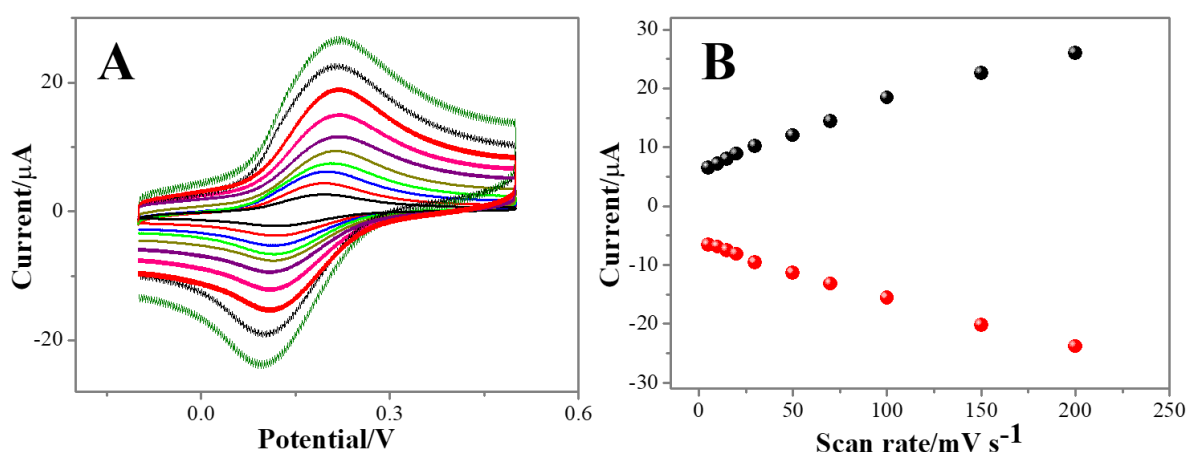


Figure 3. (A) CVs of the FePGSSs/GCE at different scan rates in pH 7.0 PBS (5, 10, 15, 20, 30, 50, 70, 100, 150 and 200 mV s^{-1} , respectively). (B) The linear dependence of peak current with the scan rate.

3.3 Optimization of experimental conditions

It is noted that this amperometric process is pH-dependent due to the nature of the carboxyl/hydroxyl groups (-COOH/-OH) and nitrogen active site on the surface of the GO/SWCNTs and PDDA, respectively [21, 22]. Therefore, to obtain an optimal current signal response, we investigated the effect of pH on the assay of the SDS and incubation time for the $[\text{Fe}(\text{CN})_6]^{3-/4-}$ anion. As shown the Figure 4A, the current signal gradually increased with the increment of pH value from pH 6.0-7.0 and then quickly decreased as the pH over 7.0. This is mainly because the -COOH/-OH groups and nitrogen active site on the surface of the PDDA/GO/SWCNTs nanocomposite are protonated-deprotonated in the highly acidic or alkaline surroundings, and therefore, the resulting damage the speed and quality of anion-exchange reaction [23]. Thus, pH 7.0 was selected as the optimum pH value for SDS detection. Meanwhile, at this pH value, the current response signal of the amperometric response signal to 5.0 mM $[\text{Fe}(\text{CN})_6]^{3-/4-}$ solution (curve a) and 100 μM SDS (curve b) increased with the increment and decreased of incubation time and leveled off after 15 min, respectively (Figure 4B). Longer incubation time did not improve the current response, thus 15 min was chosen as the incubation time for the electrochemical response signal probe and SDS detection.

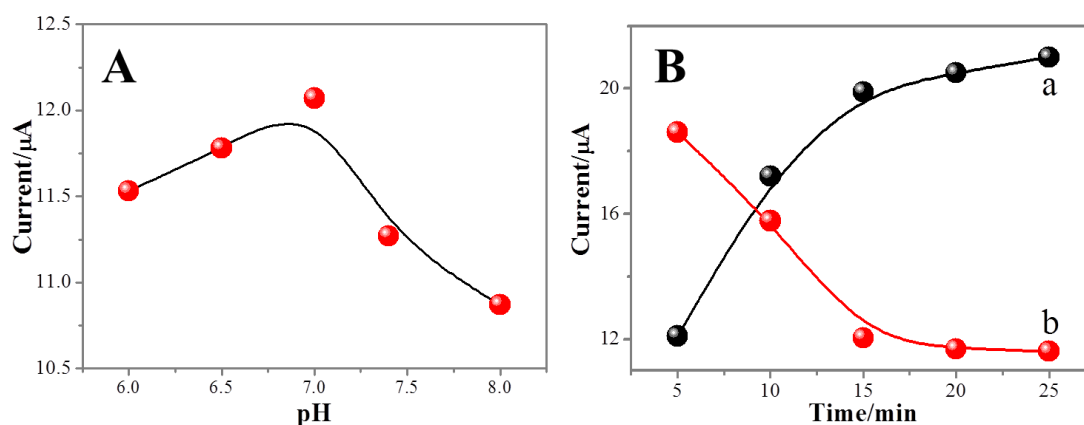


Figure 4. (A) Amperometric responses of the FePGSSs/GCE within different pH values containing 100 μM SDS at a scan rate of 100 mV s^{-1} , (B) Incubation time of PDDA/GO/SWCNTs/GCE in the 5.0 mM $\text{K}_3\text{Fe}(\text{CN})_6/\text{K}_4\text{Fe}(\text{CN})_6$ (1:1) solution (curve a) and FePGSSs/GCE in the 100 μM SDS (curve b) at a scan rate of 100 mV s^{-1} .

3.4 Amperometric SDS assay with the anion-exchange mechanism

To investigate the anion exchange feasibility between $[\text{Fe}(\text{CN})_6]^{3-/4-}$ and SDS with the PDDA as the artificial receptor, the influence of SDS on the stability of the FePGSSs-modified GCE was first investigated by CVs and differential pulse voltammograms (DPVs) (Figure 5). The black curve a in the Figure 5, depicts typical CVs and DPV obtained at the PDDA/GO/SWCNTs-modified GCE in 50 mM PBS. Prior to the confinement of $[\text{Fe}(\text{CN})_6]^{3-/4-}$ onto the electrode, the electrode shows no redox waves within the potential window employed here (Figure 5A and 5B, curve a). Upon the surface confinement of $[\text{Fe}(\text{CN})_6]^{3-/4-}$, it could be easily observed that the FePGSSs/GCE presents a well-defined cathodic and anodic peak currents at E_p of $\sim 110 \text{ mV}$ (bare GCE, $E_p=200 \text{ mV}$, Figure 5A, curve b),

which indicate that the PDDA/GO/SWCNTs modified GCE can be easily reacted with $[\text{Fe}(\text{CN})_6]^{3-/4-}$ anions by simple electrostatic adsorption [24]. Meanwhile, the redox current response of this probe was relatively stable; no tremendous change in the redox waves was observed after the FePGSSs/GCE was immersed in 50 mM PBS for 1.0 h, as shown in the inset of Figure 5A, illustrating the stable adsorption of $[\text{Fe}(\text{CN})_6]^{3-/4-}$ onto the modified electrode surface. Interestingly, when the FePGSSs/GCE was immersed into 100 μM SDS solution for 15 min, taken out of solution, and rinsed with double distilled water, the current response of the modified electrode was largely decreased in 50 mM PBS (Figure 5A and 5B, curve *c*), indicating that the $[\text{Fe}(\text{CN})_6]^{3-/4-}$ probe can be replaced by SDS through the anion-exchange mechanism. And the above results demonstrate that the stronger anion interaction should be existed between PDDA and SDS, as the guest-host interaction, SDS acted as donor and PDDA as acceptor. These observations suggest that the FePGSSs composite nano-films modified GCE can act as an electrochemical sensor for SDS detection.

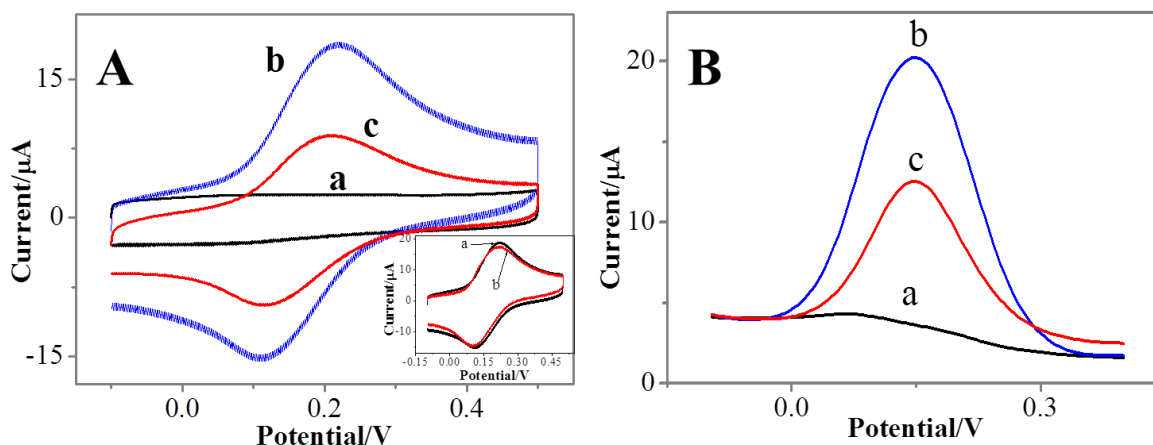


Figure 5. CVs and DPVs of PDDA/GO/SWCNTs/GCE (a), FePGSSs/GCE (b), and SDS/FePGSSs/GCE (c) in pH 7.0 PBS at a scan rate of 100 mV s^{-1} , the concentration of SDS is $100 \mu\text{M}$. Inset of the Figure 5A: Curve *a* and curve *b* represent the CVs obtained after immersing the FePGSSs/GCE in 50 mM PBS (pH 7.0) for 0 h, 1.0 h, respectively. Scan rate, 100 mV s^{-1} .

3.5 Detection of SDS based on the anion exchange on the FePGSSs-modified electrode

To evaluate the anion exchange reaction between SDS and PDDA polymer, the FePGSSs nano-films modified GCE was exposed to various concentrations (0-400 μM) of SDS solutions. Under optimal conditions, after the SDS in the sample incubated with the immobilized PDDA in the nano-films for 15 min, a DPV curve was collected (Figure 6). As shown in Figure 6A, the peak current of FePGSSs/GCE decreased gradually with the increment of SDS concentration in the sample solution, demonstrating that the sensing system is sensitive to SDS concentration. Meanwhile, to remove the background signal of the electrode-to-electrode variation, we used the ratio of current decrease (*R*) for SDS quantification by the following equation [25]:

$$R = (I_0 - I)/I_0 \times 100\%$$

where I_0 was the initial current response recorded at the FePGSSs/GCE and I was the current response at the FePGSSs/GCE after the modified electrodes were reacted with the different

concentrations of SDS. As shown in Figure 6B, with increasing the SDS concentration, the ratio of current increase was linearly increased with a dynamic linear concentration range from 1.0 to 200 μM ($y = 0.038-2.849X_{\text{SDS}} (\mu\text{M})$, $R^2 = 0.9948$) with a detection limit ($3\sigma/\text{slope}$) of 36.51 nM, (Figure 6B), which is similar with that of the previous reports based on electrochemistry and fluorescence technologies (Table 1). In short, the above results suggest that the FePGSs composite nano-films modified GCE is potentially adaptive for quantitative determination of trace SDS concentrations in an electrochemical method.

Table 1. Comparison of the method applied, specificity and LOD for SDS using different methods.

Materials used	Method applied	Linear range	LOD	Refs.
GSH-Au NCs	Fluorescence	0.2 - 12 $\mu\text{g mL}^{-1}$	0.02 $\mu\text{g mL}^{-1}$	[3]
eosin Y and PEI	Fluorescence	0.4 - 6 $\mu\text{g mL}^{-1}$	0.02 $\mu\text{g mL}^{-1}$	[1]
eosin Y and PEI	Electrochemistry	1.0 - 40 $\mu\text{g mL}^{-1}$	0.9 $\mu\text{g mL}^{-1}$	[26]
PDDA/GO/SWCNTs	Electrochemistry	0.288 - 57.6 $\mu\text{g mL}^{-1}$	0.01 $\mu\text{g mL}^{-1}$	This method

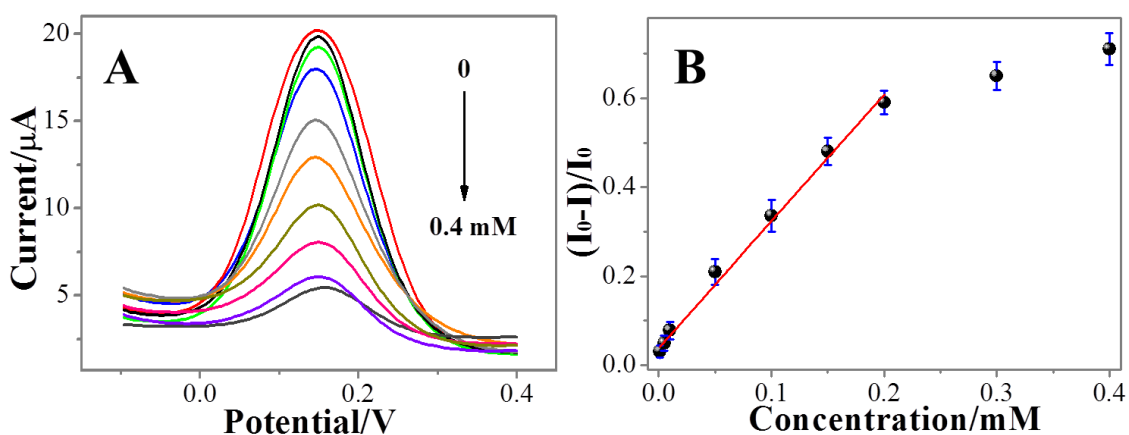


Figure 6. DPVs recorded at FePGSs/GCE in 50 mM pH 7.0 PBS after 15 min incubation into different concentrations of SDS.

3.6 Anti-interference and stability

One of the potential advantages of using SDS molecule as recognition elements in electrochemical sensors is the selectivity of the anions for its analytes. Thus, the selectivity of the present amperometric sensing system to possible interfering substances with much higher concentrations of normal level in complicated solution, including S^{2-} , F^- , Cl^- , Br^- , I^- , SDBS, NO_3^- , SO_4^{2-} , NO_2^- , PO_4^{3-} , and AcO^- was evaluated. The variable relative current intensity $[(I_0-I)/I_0]$ of the response current of the proposed amperometric sensor under the same experimental condition was compared, as shown in Figure 7. Compared with the response of much higher $[(I_0-I)/I_0]$, it is clearly seen that no prodigious increase was observed through incubation combination SDBS or other anions to the FePGSs modified GCE. This result indicated that the potential interference substances did not affect

the detection of SDS. Furthermore, these results also indicate that the fabricated electrochemical sensing platform possesses excellent specificity for SDS sensing even under the sophisticated environment.

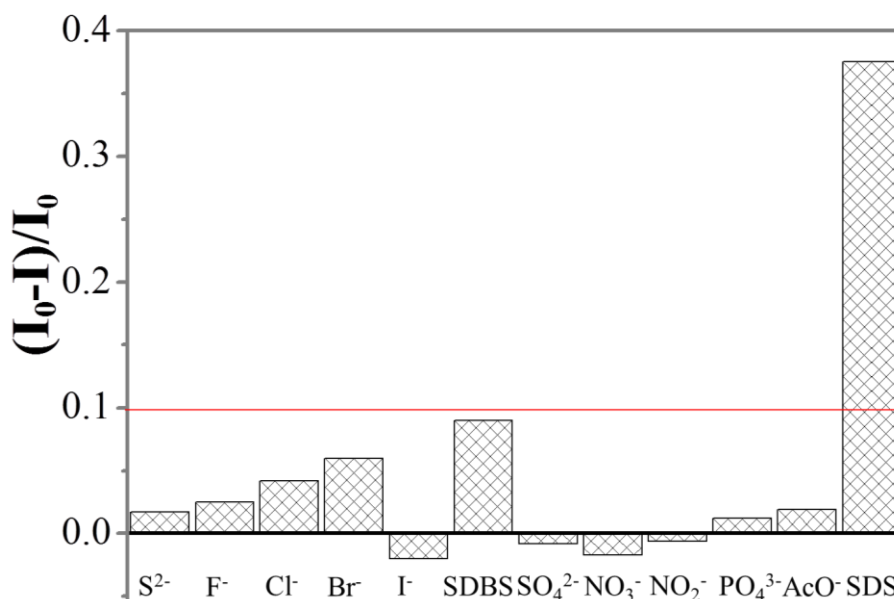


Figure 7. Selectivity of the electrochemical sensor for SDS detection. The concentration of SDS was 200 μ M and other substances were all 300 μ M.

The stability was investigated over ten days when the electrochemical sensor was stored at 4 °C. The sensor remained 94.85% of its original current after ten days, and no obvious change of the amperometric response was found over this period, indicating the effective retention of the immobilized PDDA in the hybrid nano-films. The excellent selectivity and stability of the developed sensor indicated that the 3D PDDA/GO/SWCNTs nanocomposite structure was very efficient for retaining the $[\text{Fe}(\text{CN})_6]^{3-/4-}$ in the immobilized PDDA-containing nano-films.

3.7 Analysis of real sample

To evaluate the feasibility of the proposed method for routine analysis, the validity of the method for the SDS assay in real samples was further evaluated by spiking the standard SDS solutions samples at different levels (i.e., 5, 10, and 100 μ M) into the real water samples and then analyzing the samples with the method developed in this study. The real water samples were added into 200 μ L of 50 mM PBS (pH 7.0). The obtained results are shown in Table 2. Although the addition of real samples has some influence on the conductivity of solution, good recoveries (93.60% ~ 107.60%) of SDS is still acquired. These results indicate that FePGSs/GCE modified GCE is promising for practical applications in determination of SDS in real sample.

Table 2. Determination of SDS in real water samples.

Sample	Added (μM)	Found (μM)	Recovery (%)	RSD (n=3, %)
1	5.0	5.38	107.60	4.18
2	10.0	9.36	93.60	3.59
3	100.0	96.52	96.52	4.88

4. CONCLUSIONS

By taking advantages of anion exchange principles, we have successfully demonstrated a simple and effective strategy for the amperometric assay of SDS by using PDDA polymer as the artificial receptor. And the stronger affinity between the PDDA receptor toward SDS poly-anion than toward $[\text{Fe}(\text{CN})_6]^{3-/4-}$ essentially makes our assay highly selective toward SDS sensing in the aqueous solution. Under optimum conditions, the above method displays a detection limit as low as $0.01 \mu\text{g mL}^{-1}$ (36.51 nM) for SDS and provides a good selectivity over other coexistence of substances. Meanwhile, the developed method has been successfully applied to the detection of SDS in real samples with satisfactory recoveries. All in all, the above results demonstrate that this method is simple, reliable, and practical in detecting SDS and has a great promise for environmental applications. What's more, the developed methods here provide a supplementary way to detect electrochemically inactive poly-anions.

ACKNOWLEDGEMENTS

We greatly appreciate the support of the National Natural Science Foundation of China (21705140, 21575123, 21675139, 21603184) and the Natural Science Foundation of Jiangsu Province (BK20170474), and sponsored by Qing Lan Project. And the opening project of Jiangsu Key Laboratory of Biochemistry and Biotechnology of Marine Wetland (K2016-17, K2016-20).

References

1. T. Wen, N.B. Li, and H.Q. Luo, *Anal. Chem.*, 85 (2013) 10863.
2. P.D. Purakayastha, A. Pal, and M. Bandyopadhyay, *Sep. Purif. Technol.*, 46 (2005) 129.
3. C.L. Zheng, Z.X. Ji, J. Zhang, and S.N. Ding, *Analyst*, 139 (2014) 3476.
4. L.A. Taranova, I.N. Semenchuk, T. Manolov, P.V. Iliasov, and A.N. Reshetilov, *Biosens. Bioelectron.*, 17 (2002) 635.
5. Z.P. Li, and J.R. Milton, *Anal. Chem.*, 53 (1981) 1516.
6. S.K. Sar, C. Verma, P.K. Pandey, and A. Bhui, *J. Chin. Chem. Soc.*, 56 (2009) 1250.
7. A.N. Reshetilov, I.N. Semenchuk, P.V. Iliasov, and L.A. Taranova, *Anal. Chim. Acta*, 347 (1997) 19.
8. S.N. Ding, J.F. Chen, J. Xia, Y.H. Wang, and S. Cosnier, *Electrochem. Commun.*, 34 (2013) 339.
9. N. Alexeyeva, and K. Tammeveski, *Anal. Chim. Acta*, 618 (2008) 140.
10. S.P. Jiang, Z.C. Liu, H. L. Tang, and M. Pan, *Electrochim. Acta*, 51 (2006) 5721.
11. D. Li, M.B. Muller, S. Gilje, R.B. Kaner, and G.G. Wallace, *Nat. Nanotechnol.*, 3 (2008) 101.
12. L.J. Cote, F. Kim, and J. Huang, *J. Am. Chem. Soc.*, 131 (2008) 1043.
13. R.P. Liang, Z.X. Wang, L. Zhang, and J.D. Qiu, *Sens. Actuators B Chem.*, 166-167 (2012) 569.

14. X.H. Yu, Z.X. Wang, Y.F. Gao, F.Y. Kong, W.X. Lv, H.F. Ma, and W. Wang, *Int. J. Electrochem. Sci.*, 13 (2018) 2875.
15. S.C. Tsang, Y.K. Chen, and P.J.F. Harris, *Nature*, 372 (1994) 159.
16. J.D. Qiu, L. Shi, R.P. Liang, G.C. Wang, and X.H. Xia, *Chem.-Eur. J.*, 18 (2011) 7950.
17. S. Wang, D. Yu, and L. Dai, *J. Am. Chem. Soc.*, 133 (2011) 5182.
18. S. Zhang, P. Kang, S. Ubnoske, M.K. Brennaman, N. Song, R.L. House, J.T. Glass, and T.J. Meyer, *J. Am. Chem. Soc.*, 136 (2014) 7845.
19. Z.X. Wang, J.Y. Wang, X.H. Yu, F.Y. Kong, W.J. Wang, W.X. Lv, and W. Wang, *Sens. Actuators B Chem.*, 246 (2017) 726.
20. F. Cao, S. Guo, H. Ma, D. Shan, S. Yang, and J. Gong, *Biosens. Bioelectron.*, 26 (2011) 2756.
21. M.N. Zhang, Y.M. Yan, K.P. Gong, L.Q. Mao, Z.X. Guo, and Y. Chen, *Langmuir*, 20 (2004) 8781.
22. Y. Yan, S. Shi, J. Yu, M. Zhang, Y. Zhang, H. Huang, J. Li, and Z. Jiang, *Int. J. Electrochem. Sci.*, 10 (2015) 6475.
23. S. Pandit, S. Khilari, K. Bera, D. Pradhan, and D. Das, *Chem. Eng. J.*, 257 (2014) 138.
24. H. Yao, and N. Hu, *J. Phys. Chem. B*, 114 (2010) 9926.
25. H. Qi, L. Zhang, L. Yang, P. Yu, and L. Mao, *Anal. Chem.*, 85 (2013) 3439.
26. X. Hao, J.L. Lei, N.B. Li, and H.Q. Luo, *Anal. Chim. Acta*, 852 (2014) 63.

© 2018 The Authors. Published by ESG (www.electrochemsci.org). This article is an open access article distributed under the terms and conditions of the Creative Commons Attribution license (<http://creativecommons.org/licenses/by/4.0/>).